Ivan, M., Wang, R. (2013): Anomalous high amplitude ratios of P5KP/PKPab and P4KP/P(S)cP observed globally around 1 Hz. - Journal of Seismology, 17, 2, 453-464

DOI: 10.1007/s10950-012-9330-7

Anomalous high amplitude ratios of P5KP / PKPab and P4KP / P(S)cP observed globally around 1 Hz

Marian Ivan

Department of Geophysics, University of Bucharest, 6 Traian Vuia str., 020956 Bucharest o.p.37, Romania

National Institute of Earth Physics, P.O.Box MG-21, Bucharest-Magurele, Romania

FAX: 0040212113120

marian.ivan@g.unibuc.ro

Rongjiang Wang

Helmholtz Center Potsdam, GFZ German Research Center for Geosciences, Telegrafenberg 14473, D-14473 Potsdam, Germany

wang@gfz-potsdam.de

Amplitude ratio of 30 short-period conspicuous P5KP and PKPab phases from five intermediate depth or deep events in Fiji-Tonga recorded at European stations around 150º distance shows a mean value two to three times the ratio of the synthetic amplitudes obtained by the normal-mode theory (and ak135 model) or by full-wave theory (and PREM). There is a large variance in the results, also observed in five amplitude ratios from one event in Argentina observed at temporary stations in China around 156º.

Global recordings of three major deep earthquakes in Fiji, Bonin and Western Brazil observed at ASAR, WRA and ZRNK arrays, at 59 North America stations and at six South Pole stations displayed conspicuous P4KP and PcP (or ScP) phases. The amplitude ratio values of P4KP vs P(S)cP are sometimes almost one order of magnitude larger than the corresponding values of the synthetics.

In both cases, arrival times and slowness values (corrected for ellipticity and station elevation) at the distances up to 23º beyond the A cut-off point predicted by ray theory match both the synthetics, suggesting the observations are the AB branch of PmKP (m=4,5) around one Hz. In disagreement to ray theory, no reliable BC branch is observed neither on the recordings nor on the normal-mode synthetics.

The high-amplitude ratio values cannot be explained by realistic perturbations of the velocity or attenuation values of the global models in the proximity of the core-to-mantle boundary (CMB). We speculate the focusing effects and/or strong scattering most likely associated to some anomalous velocity areas of the lowermost mantle are responsible for that.

The results suggest limitations of the previous evaluations of the short-period attenuation in the outer core from PmKP amplitudes (m>=3), irrespective of the fact that they are obtained by using ray theory, normal-mode or full-wave synthetics. Attempts to use PmKP arrival times in order to refine velocity structure in the proximity of CMB should be also regarded with care if the propagation times have been computed with ray theory.

BC and AB PmKP-branches, amplitude ratio, slowness, CMB, full-wave theory, normal-mode synthetics, outer core

1 Introduction

Ray theory (e.g. Crotwell et al., 1999) routinely predicts two branches (BC and AB) for PmKP (m>=2) core phases, multiple reflected by the inner side of the core-to-mantle boundary (CMB). For m=4, the slowness of $P4KP_{BC}$ branch, having the bouncing point deeper located in the outer core (OC), slightly decrease from around 4.3 s/deg to 2.2 s/deg. That phase should be theoretically observed from epicentral distances around 41º (the position of the cusp point B) up to antipodal position of C point. The $P4KP_{AB}$ branch (with a shallow bouncing point in the OC) should be recorded up to an epicentral distance around 54 deg (i.e. the position of the cut-off point A). Its slowness increases from 4.3 s/deg to 4.45 s/deg, the last value corresponding to the diffraction on CMB.

For P5KP, the cusp point B is located close to 122º, while the cut-off point A is around 133º. The above positions of the cusp/cut-off points only slightly depends on the global model used in computations and on the focal depth.

Engdahl (1968) was the first to identify such multiple reflections within the Earth's core, suggesting their importance in estimating the properties of the CMB and the value of the attenuation factor Q_P in the OC. For m>=3, he mentioned that the observations beyond the cut-off point A better match the AB branch, probably due to the high value of the reflection coefficient on CMB. Adams (1972) assumed that the absence of the BC branch was the result of a severe amplitude decrease at each internal reflection of P3KP or P4KP, due to steeper incidence angles at CMB. A further possible explanation has been suggested by Qamar and Eisenberg (1974). They proposed that the decrease of the amplitude was due to geometrical spreading.

Observations of P2KPab about 7.5º past the ray theoretical cutoff distances have been interpreted by Rost and Garnero (2006) as diffraction along the major arc and used to map ultralow velocity zones of the lowermost mantle. Because PmKP

waves are piercing CMB at near-grazing incidence, Richards (1973) and Cormier and Richards (1976) underlined the necessity of using full-wave theory in evaluation of the amplitudes, especially considering the high-frequency content (around 1 Hz) of such phases. However, full-wave theory itself cannot predict the arrival times/slowness, but only the amplitudes of PmKP.

Short-period attenuation in the OC attenuation has been estimated by using the amplitude (spectral) ratio method and ray theory applied to various pairs of phases, providing a large range of the results. Sacks (1971) used P'P' vs P, obtaining a minimum Q_P of 3000 (in agreement to the lower value of 2200 of Adams (1972)) and a more confident value of 10,000. From amplitude ratios of P3KP, P4KP and P5KP, Buchbinder (1971, 1972) determined a Q_P value around 4000 and estimated travel times and velocities in OC. Qamar and Eisenberg (1974) reported a short-period Q_P in the range 5000-10,000 from P7KP vs P4KP. Various global models actually assume extremely low attenuation in the OC (e.g. Q_P = 57822 for ak135 model (Montagner and Kennett 1996)). That value is based mainly on Earth's free oscillations. Recent reports (e.g. Helffrich and Kaneshima 2004) indicate that the attenuation in the OC is constant and low, with no evidence for layering, except the lowermost OC (e.g. Zou et al. 2008; Cormier 2009).

Several previous studies reported anomalous amplitudes ratio of various phases. Schweitzer and Müller (1986) observed low amplitude ratios SKS-to-SKKS for Tonga-Fiji events recorded at American stations, probably because of strong horizontal S-velocity gradients in the lower mantle on the source side, confirmed by the tomographic models (e.g. Masters et al. 2000). Large variations of PcP-to-P amplitudes at Canadian Yellowknife array YKA for earthquakes in Western Aleutians have been reported by Rost and Revenaugh (2004), with some values more than one order of magnitude larger than predicted by PREM or IASP91 models. Following an extensive discussion of various mechanisms able to produce such observations, their preferred interpretation is based on small-scale variations of the CMB reflection coefficient beneath the Alaskan Kenai Peninsula.

Herein, we report an observed amplitude ratio of conspicuous P5KP vs PKPab and P4KP vs PcP (or ScP) recorded globally around 1 Hz for major, deep events in Bonin, Fiji-Tonga and South America. Arrival times and amplitudes are compared to the synthetics evaluated by normal-mode theory (Gilbert and Backus

1968; Takeuchi and Saito 1972) and the orthonormalized matrix algorithm of Wang (1999), for numerical stability. For P5KP vs PKPab, synthetics have been also evaluated by the full-wave theory and Langer's approximation (Cormier and Richards 1977, 1988) using PREM model. Both the slowness and the propagation times of the normal-mode synthetics fully match the observations, but no significant energy is observed in relation to the BC branch predicted by ray theory. However, anomalous high amplitudes of the P5KP vs PKPab or P4KP vs P(S)cP are observed. We speculate they indicate strong focusing effects and/or scattering, most likely located in the area of the piercing points on CMB of both PmKP and the reference phases.

Given the anomalous observed amplitudes around 1 Hz, previous results on the short-period attenuation factor Q_P in the OC obtained from amplitudes of PmKP should be treated with caution, irrespective of the fact that they have been derived with full-wave or ray theory. When PmKP phases are used to refine velocity structure in the proximity of CMB, propagation times are better to be computed with normal-mode synthetics rather than using ray theory.

2 Observations

In order to minimize scattering of the short-period amplitude phases (~1 Hz) inside the crust or upper mantle and the waste of high energy there, only major intermediate depths or deep events have been examined (Table 1 and Figure 1) for conspicuous PmKP (m=4,5) and for the reference phases. For each event, a careful examination of the ISC Bulletin was performed in order to avoid the misinterpretation of PmKP by phases related to aftershocks or to other earthquakes, eventually located in the proximity of the source-to-receiver path. For P5KP, we consider PKPab as a reference phase. For P4KP, the reference phase is PcP. If PcP has not been observed with a high signal-to-noise ratio (SNR), ScP has been used as reference. In that situation, the distance between P4KP and ScP piercing points on CMB is theoretically expected to be larger. Figure 2 illustrates the very similar path into the mantle for the PnKP and the reference phases. However, the branch of the core phases here is BC, ray theory indicating no AB branch at such epicentral distances. Further evidence is that the last branch is most likely present in our observations.

The investigated earthquakes show a variety of focal mechanisms, but a simple faulting process.To date, only the 2002/10/12 W. Brazil earthquake displays a complex source time function, with a small forerunner preceding the main event by around 2.5 seconds. It is observed for all P, PcP and P4KP waveforms.

The P5KP observations are from four earthquakes in the Tonga-Fiji zone recorded at European stations and an event in Argentina recorded at Tibet stations.

Observations of P4KP came from one earthquake in Bonin area (1996/03/16) recorded at ASAR and at ZRNK arrays. The 2002/10/12 W. Brazil earthquake provided conspicuous P4KP and PcP recordings at 59 North American stations with a rather large azimuth range.

The 2000/12/18 Fiji event provided both P5KP and P4KP observations. The first phase was recorded at several European stations, while the last one, at ASAR, WRA and at some South Pole stations. In the final case, ScP was used as reference phase.

Data have been obtained from Incorporated Research Institutions for Seismology (IRIS) (permanent stations as well as temporary ones from the INDEPTH II Project), from the German SZGRF network and from the GEOFON Data Center (permanent stations as well as temporary ones from Eifel Plume Project).

3 Waveform processing

All the P5KP broad-band data has been filtered to a WWSSN short-period instrument, which seems to be best suited for recording of such core phases (Bormann et al. 2002) and Hilbert transformed for better identification of the PKPab arrival. This is particularly necessary for distances around 147°, where the interference with PKPbc might render more difficult the exact identification of the PKPab arrival.

For all the P4KP and PcP recordings, filtering of the broad-band data to a short-period S-13 sensor with a natural frequency around 1 Hz proved to be the most appropriate. No filtering has been used for other short-period recording sensors (e.g. Geotech 23900, Mark L-4c, Kinemetrics Ranger SS-1), as their instrument response is quite similar to S-13, at least around 1 Hz.

In all cases, the PmKP and the reference phases (PKPab or P(S)cP) have been identified based on their frequency content (around 1 Hz), impulsive onset, conspicuous amplitude above noise and arrival times in the proximity of the values evaluated with TauP Toolkit and ak135 model (Crotwell et al 1999). An example of P5KP recordings reduced by the Pdif slowness is presented in Figure 3, with the corresponding vespagram. By correlation of wave peaks or troughs between stations, relative arrival times have been obtained, and slowness has been evaluated by fitting a straight line. A comparison between observed and theoretical arrival times of both BC and AB branches of PmKP (m=4,5) is presented in Figure 4. A vespagram of P4KP arrivals is further illustrated in Figure 5.

Synthetic seismograms have been computed using normal mode theory, for the Harvard CMT parameters of each event and the ak135 model. Such long-period focal mechanisms could be slightly different from the solutions obtained from short-period recordings (Rost and Revenaugh 2004). However, differences between the take-off angles of P5KP and PKPab are less than 5 ° and the variations in the ratio of the far-field radiation patterns (P5KP vs PKPab) are below 3% for all the events / stations in Table 1. The situation is quite similar to P4KP and PcP. Use of ScP as a reference phase for P4KP provides less reliable results than considering the increased distance between their CMB piercing (reflection) points.

Peak-to-trough amplitudes have been evaluated for both the recordings and the synthetics (the last ones also filtered to a WWSSN_SP or S-13 instrument, respectively) and resampled to 8 Hz (sampling frequency of the synthetics). Routinely, both PmKP and the reference phases display a very narrow frequency band, as being represented by only two or three half-cycles with a period slightly above 1 s.

Good SNR examples are presented in Figure 6 and 7. If the PmKP and/or the reference phase waveforms (synthetics or recordings) displayed more than three half-cycles above the noise, their amplitudes have been measured for each peak-to-trough pair, and an error has been ascribed to in each case. Finally, the amplitude ratio of P5KP vs. PKPab and P4KP vs PcP (or ScP) has been evaluated, and several numerical tests performed by realistic modification of the ak135 model parameters in the proximity of the CMB.

4 Results and discussion

The observed minus computed (O-C) arrival times of PmKP are around 12 s when the computations are performed using the ray theory and TauP method (Crotwell et al. 1999), which predicts the existing of only the BC branch at most distances in this study. Such differences cannot be explained by ellipticity/asphericity corrections (Doornbos 1988), which are around 1-2 s. However, the observed PmKP arrival times are very closed to the normal-mode synthetics.

The observed slowness values are listed in Table 2 with their 95% errors (Draper and Smith 1966). There is a relative large variance (standard deviation of ± 0.16 s/deg) for the six slowness estimation of P5KP, most likely associated to mantle heterogeneities along the wave path, but in agreement to other estimations of Pdif slowness (see a synopsis in Wysession et al. 1992). The mean average of the slowness is 4.47 s/deg, very closed to the value of the 4.45 s/deg predicted by various global models for the AB branch near the cusp point B, or to the theoretical slowness of Pdif.

Amplitude results are presented in Table 3 and Figure 8 for P5KP, showing an increased variance at distances below 150º, most likely due to the contamination of PKPab by PKPbc branch coda. Ignoring the extreme high values (associated routinely to lower SNR), the observed amplitude ratios also exceed the synthetic ones, by a factor of approximately two in the case of the five events from Fiji recorded by the European stations. There is a large variance of the results which cannot be exclusively associated to the noise level. The amplitude values of the normal-mode synthetics (and ak135 model) are very close to the theoretical values provided by the full-wave / Langer's approximation theory (and PREM).
Given the close slowness values of the P5KP and reference phases, the high-amplitude ratios in respect to the synthetics are difficult to explain by near-source (receiver) or upper mantle inhomogeneities (see a detailed discussion by Rost and Revenaugh (2004)). Realistic perturbations of the properties in the proximity of the CMB cannot cause such anomalous values. For example, an increase of the P-wave velocity immediately above CMB by 10% (from 13.66 to 15.03 km/s in ak135 model) modifies the amplitude of P5KP synthetics by around 67%. Decreasing the density just below CMB by 20% (from 9.91 to 7.96 g/cm^3) also increases P5KP amplitude by another 23%, but a precursor of the P5KP is clearly

observed in synthetics but not in real data. Such changes lead to only minor variations in the PKPab reference phase amplitude. In fact, a significant decrease of velocity immediately below CMB also predicts a well-individualized arrival of S3KS in respect to SKS and SKKS, not seen in observations (Schweitzer and Müller 1986).

Simulating the 1998/03/29 event at AQU station, a double attenuation value in OC (QP= 28911) decreases PKPab by around 2% and P5KP by 9%, without changing the pulse widths. So, both amplitude ratios or pulse width techniques are passive to realistic changes of the OC attenuation.

The observed amplitude ratios P4KP vs PcP (or ScP) are presented in Table 4, indicating in some cases highly anomalous values when compared to the synthetics. A map of the P4KP/PcP amplitude ratios observed at the North American stations for the 2002/10/12 event is presented in Figure 9, suggesting a large regional anomaly, with amplitude ratios almost one-magnitude order higher than the synthetics in the central part of the area. Again, such anomalous values cannot be explained by realistic perturbations of the global model in the proximity of the CMB or by replacing the ak135 model to PREM or IASPEI91. Increasing the P-wave velocity immediately above CMB by 10% in the ak 135 model increases the P4KP/PcP amplitude ratio of the synthetics by less than 20% for a station at 55°.

Note that PcP vs P amplitudes are also higher than normal for that event (Fig. 10), while the PcP vs P amplitude ratio of the synthetics is only slightly varying from 0.26 at a station like TXAR (Δ=48.5°) to 0.18 at a distance Δ=63.6° like NVAR.

Similar behavior seems also to apply to the PKPab vs PKPbc amplitude ratio of the observations, which seems to be higher than the corresponding synthetics (see Fig. 6).

Our observation of impulsive PmKP with the energy being highly focused around 1s at distances like 20° or more beyond the cut-off point cannot be satisfactorily explained by a simple diffraction mechanism. Routinely, at such distances, Pdif is a very emergent, long period phase, best observed in long-period (> 10 s) recordings (see Astiz et al. 1996).

So, we believe that a mechanism involving focusing and/or strong scattering (e.g. Kampfmann and Müller 1989; Bataille and Lund 1996; Vidale and Hedlin

1998) is responsible for our anomalous amplitude observations. At least for P5KP recordings at European stations of Fiji earthquakes, such focusing areas appear to be associated to the root of the Central Pacific super plume (Romanowicz and Gung 2002). Observations at North America stations of the 2002/10/12 event in Western Brazil also have the piercing points of the P4KP phases located in the very proximity of areas where intense scattering in the lower mantle has previously been reported by Tibuleac and Herrin (1999).

The anomalous amplitudes' observations suggest that previous results on the short-period attenuation factor Q_P in the OC obtained from amplitudes of PmKP should be treated cautiously, irrespective of the fact that they have been derived with full-wave or ray theory. The relatively large variance in the amplitudes of PmKP and the reference phase having similar paths in the mantle, suggest that several results based on other phases interacting with CMB but having larger distances between their CMB piercing points should also be regarded with care (e.g. Koper and Pyle 2004).

The variance of the PKP amplitudes around 1 Hz could also partially explain the large range in the Q_P attenuation factor in the inner core obtained with spectral ratio method (routinely performed in the frequency band 0.2 to 2 Hz). It is usually assumed to be the result of a mosaic-like structure at the inner-core boundary (Krasnoshchekov et al. 2005) or of strong heterogeneity at the base of the mantle (Bowers et al. 2000). It could also explain the exception of linearity in the frequency spectra of PKPbc vs. PKPdf observed by Souriau and Roudil (1995) for some paths from southwest Pacific events to Western European stations.

Finally, we note that no reliable conspicuous forerunners or post-cursors of PmKP have been observed in this study, in agreement to Helffrich and Kaneshima (2004).

5 Conclusions

Two branches, BC and AB are predicted by ray theory for the seismic waves multiple reflected within Earth's outer core. In this study, no reliable presence of the BC branch of PmKP (m=4 or 5) could be observed in neither recordings nor normal-mode synthetics. The observed arrival times and slowness values suggest that the observations are the AB branch of PmKP, in agreement to the supposition of Engdahl (1968) or Adams (1972) on other multiple core reflections.

Consequently, attempts to use PmKP in order to refine velocity structure in the proximity of CMB should use the propagation times computed with normal-mode synthetics. This is of particular importance for observations performed beyond the cut-off point A. Here, the differences between travel times computed with ray theory and normal-mode synthetics can reach 10 s or more.

Most of the PmKP observations show anomalous high amplitude ratios when compared to reference phases having a very similar path in the mantle. Such amplitudes cannot be explained by realistic changes of the global models parameters near CMB. Hence, attempts to use PmKP amplitudes in order to estimate short-period (around 1 Hz) attenuation factor Q_P in the outer core should be regarded with care.

Acknowledgements

Dr. S. Wendt (University of Leipzig) kindly provided details about core phases recorded at German Seismological Network. Professor V.F. Cormier is acknowledged for providing schairy code for evaluating synthetics with Langer's approximation and PREM model. IRIS, GEOFON and German SZGRF Data Centers are acknowledged for providing the waveform data. We thank Pawel Wiejacz and two anonymous reviewers for constructive and critical comments that have improved the manuscript. GMT files (Wessel and Smith 1996) have been used to prepare some of the diagrams.

References

Adams RD (1972) Multiple inner core reflections from a Novaya Zemlya explosion. Bull Seismol Soc 62: 1063-1071

Astiz L, Earle PS, Shearer PM (1996) Global Stacking of Broadband Seismograms, Seismo Res Lett 67: 8-18

Bataille K, Lund F (1996) Strong scattering of short-period seismic waves by the core-mantle boundary and the P-diffracted wave. Geophys Res Lett 23: 2413-2416

Bormann P, Klinge K, Wendt S (2002) Ch. 11: Data Analysis and Seismogram Interpretation. In: Bormann, P. (Ed.) IASPEI New Manual of Seismological Observatory Practice, GeoForschungsZentrum Potsdam, vol. 1, 89–98

Bowers D, McCormack DA, Sharrock DS (2000) Observations of PKP(DF) and PKP(BC) across the United Kingdom: implications for studies of attenuation in the Earth's core. Geophys J Int 140: 374-384

Buchbinder GGR (1971) A velocity structure of the earth's core. Bull Seismol Soc Amer 61: 429-456

Buchbinder GGR (1972) Travel times and velocities in the outer core from PmKP. Earth Planet. Sci. Lett., 14,161-168.

Cormier VF, Richards PG (1976) Comments on 'The Damping of Core Waves' by Anthony Qamar and Alfredo Eisenberg. J Geophys Res 81: 3066-3068
Cormier VF, Richards P (1977) Full wave theory applied to a discontinuous velocity increase: The inner core boundary. J Geophys Res 43: 3-31
Cormier VF, Richards P (1988) Spectral synthesis of body waves in earth models specified by vertically varying layers, in Seismological Algorithms, Computational Methods and Computer Programs, edited by D.J. Dornboos, 3-45, Academic Press, London and New York
Cormier VF (2009) A glassy lowermost outer core. Geophys J Int 179: 374-380
Crotwell H P, Owens TJ, Ritsema J (1999) The TauP Toolkit: Flexible seismic travel-time and ray-path utilities. Seism Res Lett 70: 154–160
Doornbos DJ (1988) Asphericity and Ellipicity Corrections, in: Seismological Algorithms, Computational Methods and Computer Programs, edited by D.J. Dornboos, 75–85, Academic Press, London and New York
Draper NR, Smith H (1966) Applied Regression Analysis. John Wiley and Sons, New York
Engdahl ER (1968) Seismic Waves within Eart's Outer Core: Multiple Reflection. Science 161:263-264
Gilbert F, Backus GE (1966) Propagator matrices in elastic and vibration problems. Geophysics 31: 326-332
Helffrich G, Kaneshima S (2004) Seismological Constraints on Core Composition from Fe-O-S Liquid Immiscibility. Science 306: 2239-2242
International Seismological Centre, *On-line Bulletin*, http://www.isc.ac.uk, Internatl. Seis. Cent., Thatcham, United Kingdom, 2010.
Kampfmann W, Müller G (1989) PcP amplitude calculations for a core-mantle boundary with topography. Geophys Res Lett 16: 653-656
Koper KD, Pyle ML (2004) Observations of PKiKP/PcP amplitude ratios and implications for Earth structure at the boundaries of the liquid core. J Geophys Res 109: 1-13
Krasnoshchekov DN, Kaazik PB, Ovtchinnikov VM (2005) Seismological evidence for mosaic structure of the surface of the Earth's inner core. Nature 435: 483-487
Masters G, Laske G, Bolton H, Dziewonski A (2000) The Relative Behavior of Shear Velocity, Bulk Sound Speed, and Compressional Velocity in the Mantle: Implications for Chemical and Thermal Structure in: Earth's Deep Interior Mineral Physics and Tomography From the Atomic to the Global Scale, Vol. 117: Geophysical Monograph Series, pp. 63–87, eds
Karato S, Forte A, Liebermann R, Masters G, Stixrude L, American Geophysical Union
Montagner J-P, Kennett BLN (1996) How to reconcile body-wave and normal-modes reference Earth models. Geophys J Int 125: 229-248
Qamar A, Eisenberg A (1974) The Damping of the Core Waves. J Geophys Res 79: 758-765
Richards PG (1973) Calculation of body waves, for caustics and tunneling in core waves. Geophys J Roy Astron Soc 35: 243-264
Romanowicz B, Gung Y (2002) Superplumes from the Core-Mantle Boundary to the Lithosphere: Implications for Heat Flux. Science 296: 513-516

Rost S, Garnero EJ (2006) Detection of an ultralow velocity zone at the core-mantle boundary using diffracted $PKKP_{ab}$ waves. J Geophys Res 111, B07309, doi:10.1029/2005JB003850
Rost S, Revenaugh J (2004) Small-scale changes of core-mantle boundary reflectivity studied using core reflected PcP. Phys Earth Planet Int 145: 19-36
Sacks IS (1971) Anelasticity of the outer core. Annu Rep Dir Dep Terr Magn 1969-1970, p 414, Carnegie Inst, Washington D.C.
Schweitzer J, Műller G (1986) Anomalous difference traveltimes and amplitude ratios of SKS and SKKS from Tonga-Fiji events. Geophys Res Lett 13: 1529-1532
Souriau A, Roudil P (1995) Attenuation in the uppermost inner core from broad-band GEOSCOPE PKP data. Geophys J Int 123: 572-587
Takeuchi H, Saito M (1972) Seismic surface waves. In: Bolt, B.A. (Ed.) Seismology: Surface Waves and Earth Oscillations, Methods in Computational Physics, v.11, 217-295. New York, Academic Press
Tibuleac IM, Herrin E (1999) Lower mantle heterogeneity beneath the Caribbean sea. Science 285: 1711-1715
Vidale JE, Hedlin M (1998) Intense scattering at the core-mantle boundary north of Tonga: evidence for partial melt. Nature 391: 682-685
Wang R (1999) A simple orthonormalization method for the stable and efficient computation of Green's functions. Bull Seismol Soc Amer 89: 733-741
Wessel P, Smith WHF (1996) A global, self-consistent, hierarchical, high-resolution shoreline database. J Geophys Res 101:8741–8743
Wysession ME, Okal EA, Bina CR (1992) The Structure of the Core-Mantle Boundary From Diffracted Waves. J Geophys Res 97: 8749-8764
Zou Z, Koper K, Cormier VF (2008) The structure of the base of the outer core inferred from seismic waves diffracted around the inner core. J Geophys Res doi:10.1029/2007JB005316

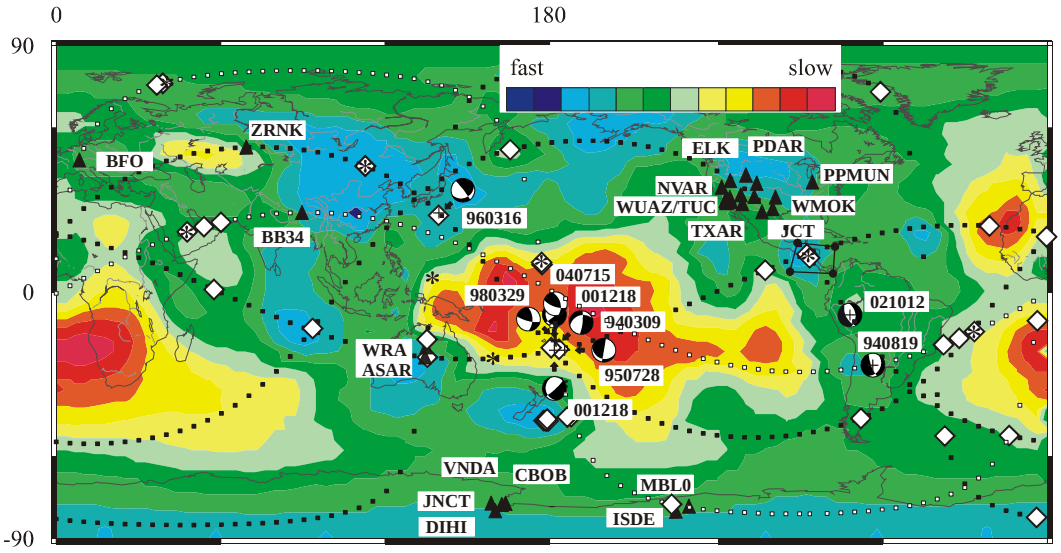

Fig. 1 Some representative paths of the events used in this study. Diamonds and stars indicate PmKP, respectively the reference phases PKPab or P(S)cP piercing points to CMB. The quadrilateral beneath Central America shows the approximate locations of PcP reflection points from 2002/10/12 event to North America stations. The background is represented by the Scripps lowermost mantle tomographic model SB4L18 (Masters et al. 2000). The beach-balls are Harvard CMT solutions.

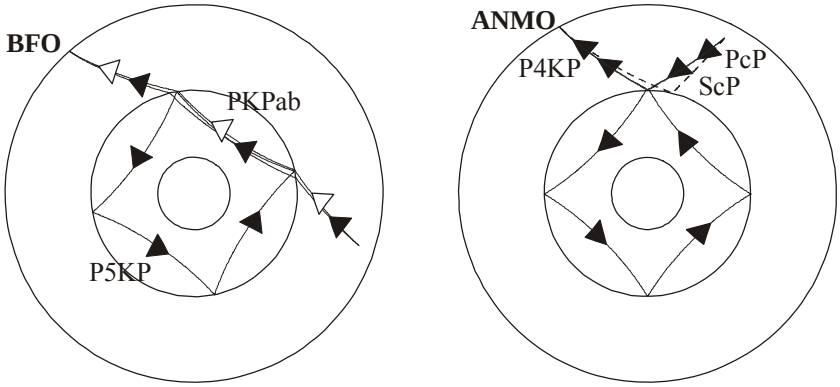

Fig. 2 P5KP and PKPab path for an event at 537.2 km depth to a station at 148.7 ° (left) and P4KP and P(S)cP path from an event at 534 km depth to a station at 54.2° (right). PmKP is the ray-theory BC branches.

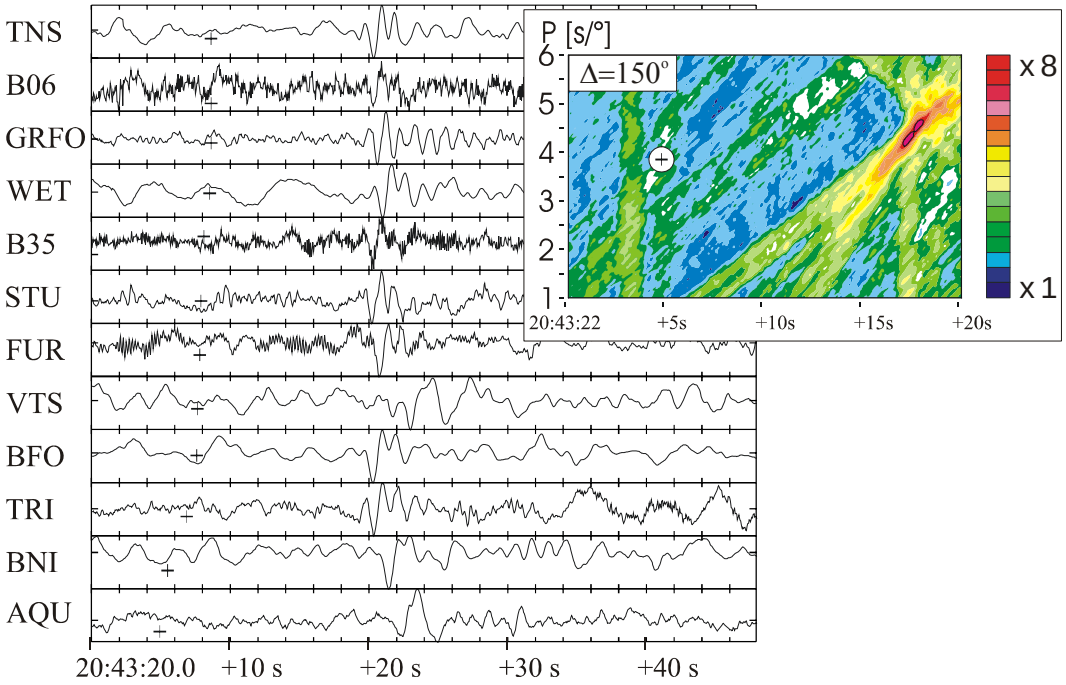

Fig. 3 P5KP recordings of 1998/03/29 event at several European stations reduced for a Pdif slowness of 4.446 s/deg at 150° epicentral distance. The inset shows the corresponding vespagram obtained for the envelope of the recordings. The cross corresponds to the theoretical BC branch.

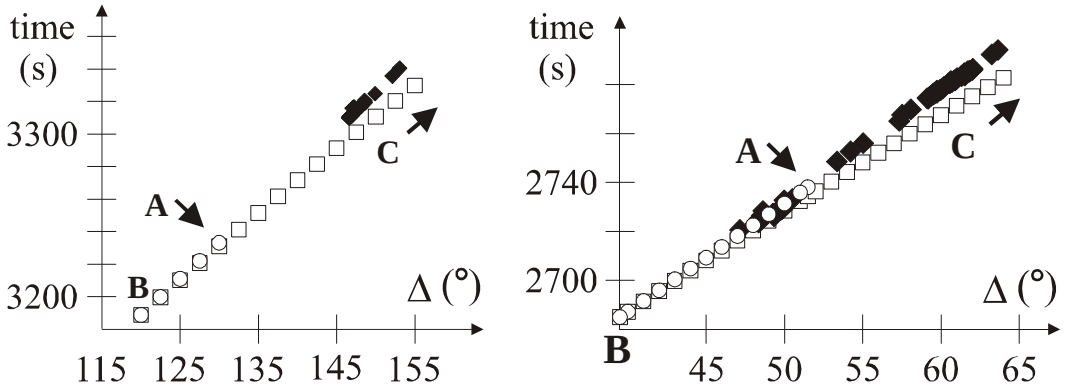

Fig. 4 Theoretical propagation time (ray theory) of P5KP branches for an event at 537.2 km depth (ray theory, AB branch - white circles, BC branch – white squares) and observations (black diamonds, corrected for ellipticity and station elevation) of 1998/03/29 event at European stations (left). Same caption for the P4KP branches of a 534 km depth earthquake and observations of the 2002/10/12 event at the 59 North America stations (right). The cusp point B and the other points are identified according to the common usage (e.g. Engdahl, 1968).

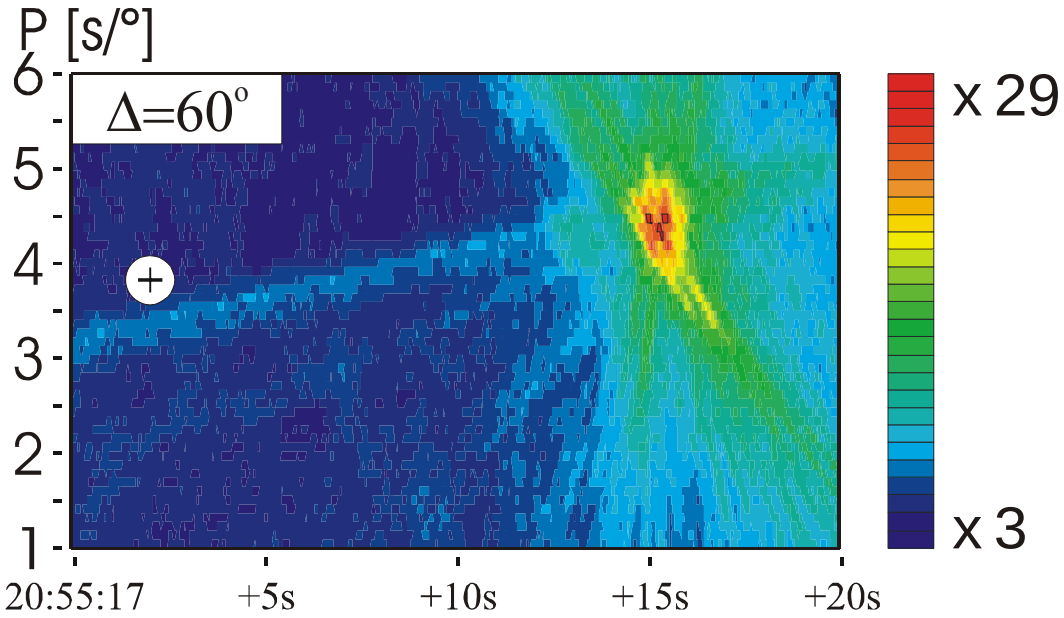

Fig. 5 P4KP vespagram for the 59 recordings at North America stations (in the distance range 47º-64º) of the Western Brazil 2002/10/12 event, corrected for ellipticity and elevation. All the broad-band recordings have been filtered to a S-13 instrument and resampled to 20 Hz. The cross shows the theoretical slowness / arrival time evaluated with ray-theory for the BC branch. Reduction distance is 60º.

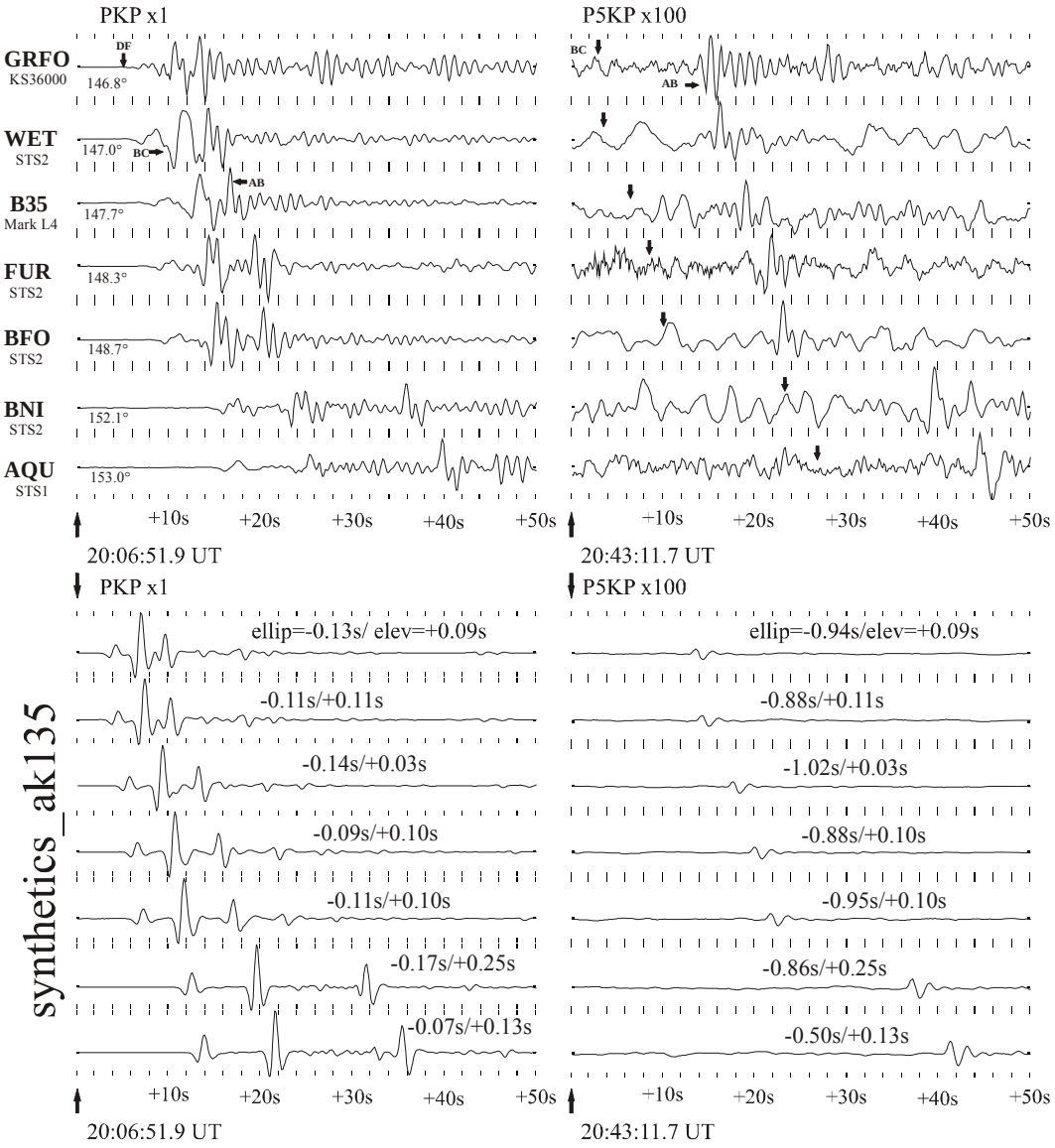

Fig. 6 Vertical component recordings (top) and normal-mode theory synthetics (bottom) of 1998/03/29 Fiji event (see Table 1 for details). Amplitude scale of P5KP traces (right) is 100 times greater than the corresponding scale of PKP (left). Arrows indicate DF, BC and AB branches. All traces are WWSSN_SP filtered, and Hilbert transformed. Sampling interval is 8 Hz for all traces. Figures on the synthetics indicate ellipticity (ellip) and station elevation (elev) corrections for the PKPab and for P5KPbc branches, to be add to the arrival times of the synthetics.

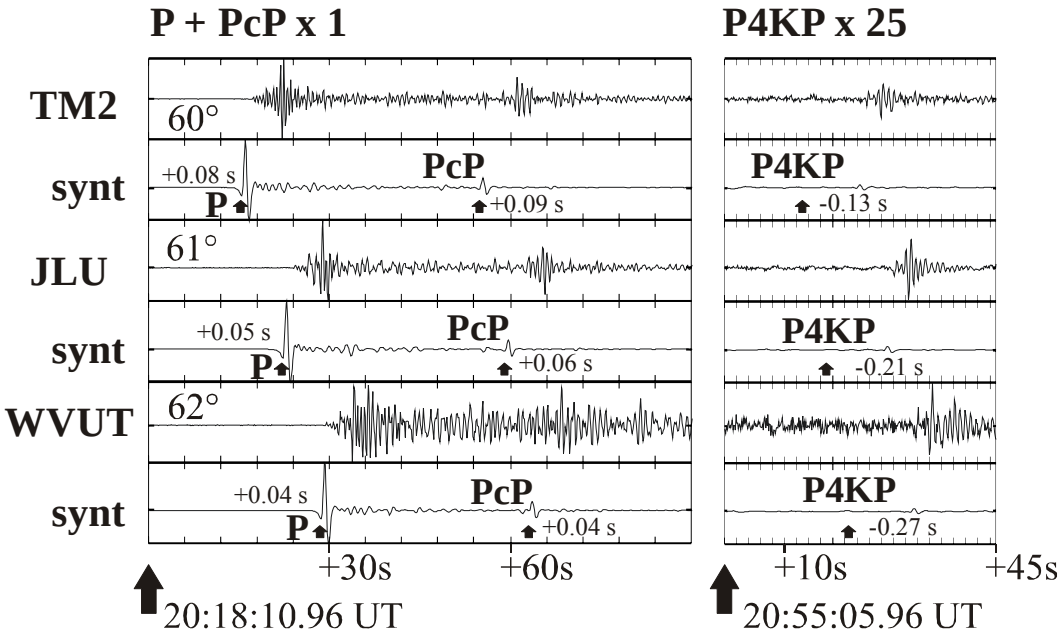

Fig. 7 Vertical component recordings of Western Brazil 2002/10/12 event (with a complex source) to several North America stations. Corresponding synthetics are below each trace. Guralp CMG 3ESP broad-band recording at JLU has been filtered to a Geotech S-13 instrument. Raw recordings are presented at TM2 (S-13 at 1 Hz) and WVUT (Mark Products L-4c). Amplitude scale of P4KP traces (right) is 25 times greater than the corresponding scale of PKP (left). Arrows indicate the arrival times predicted by ray theory (for the BC branch) and figures in their proximity are the ellipticity corrections.

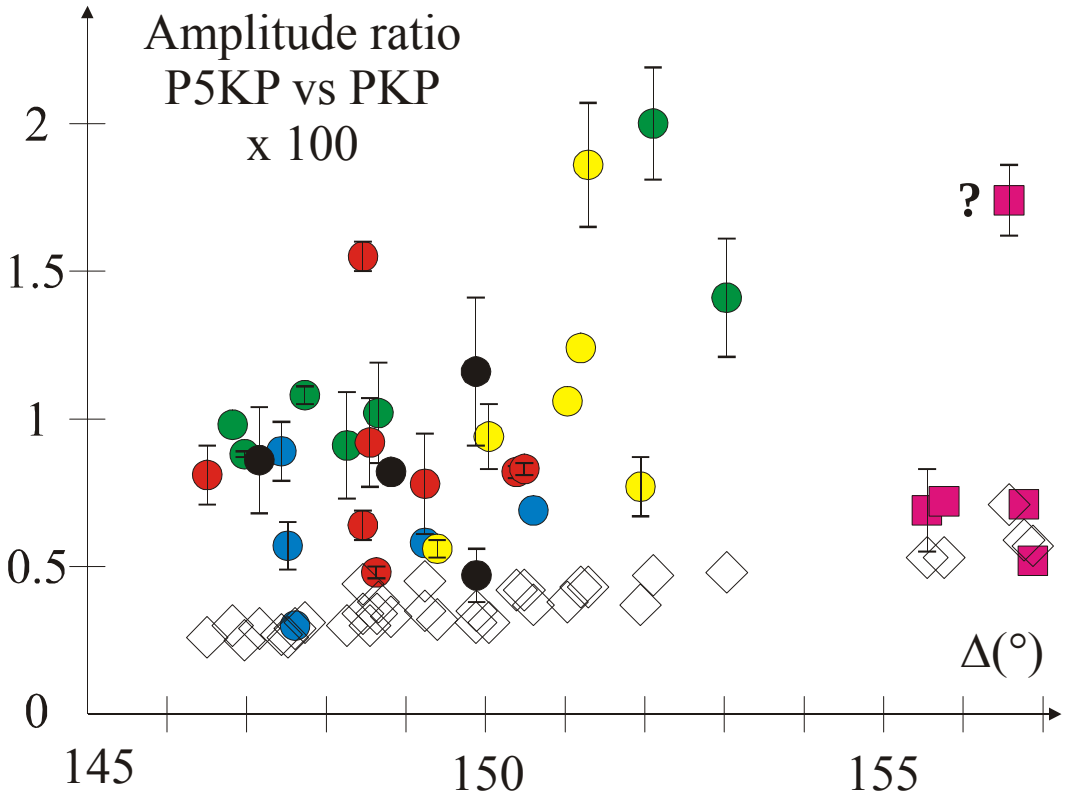

Fig. 8 Amplitude ratio observations of P5KP/PKBab from Fiji events to European stations (circles) and Argentina to Tibet (squares). The diamonds are the amplitude ratio of the corresponding synthetics. The question mark indicates a low signal-to-noise ratio.

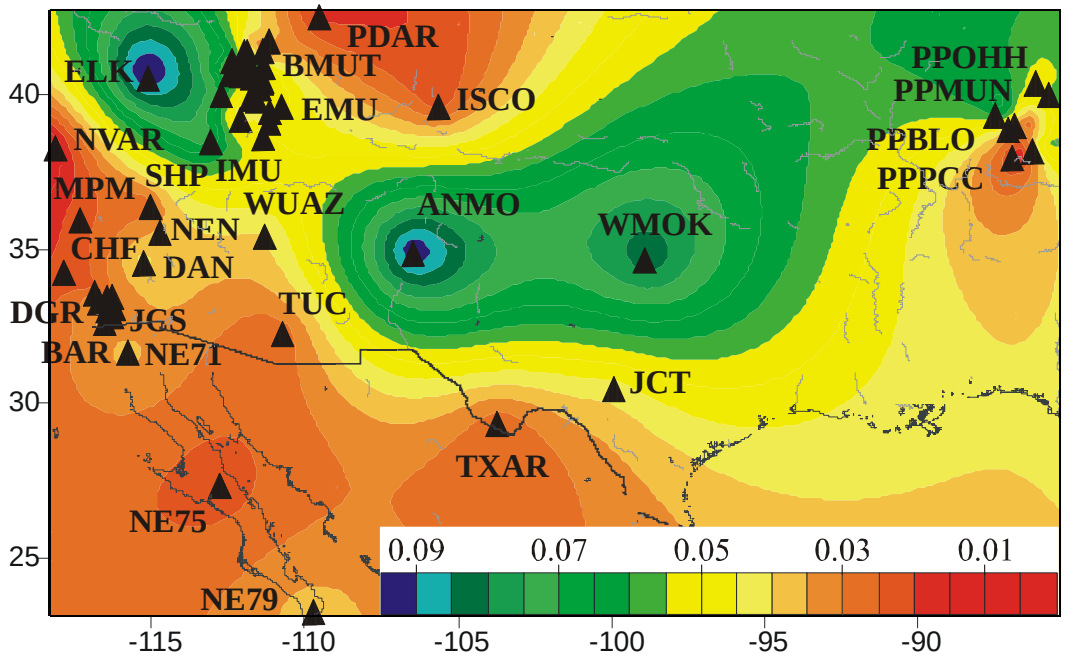

Fig. 9 Observed amplitude ratio values of P4KP/PcP at the North American stations for 2002/10/12 event in West Brazil. Kriging interpolation with a medium smoothing.

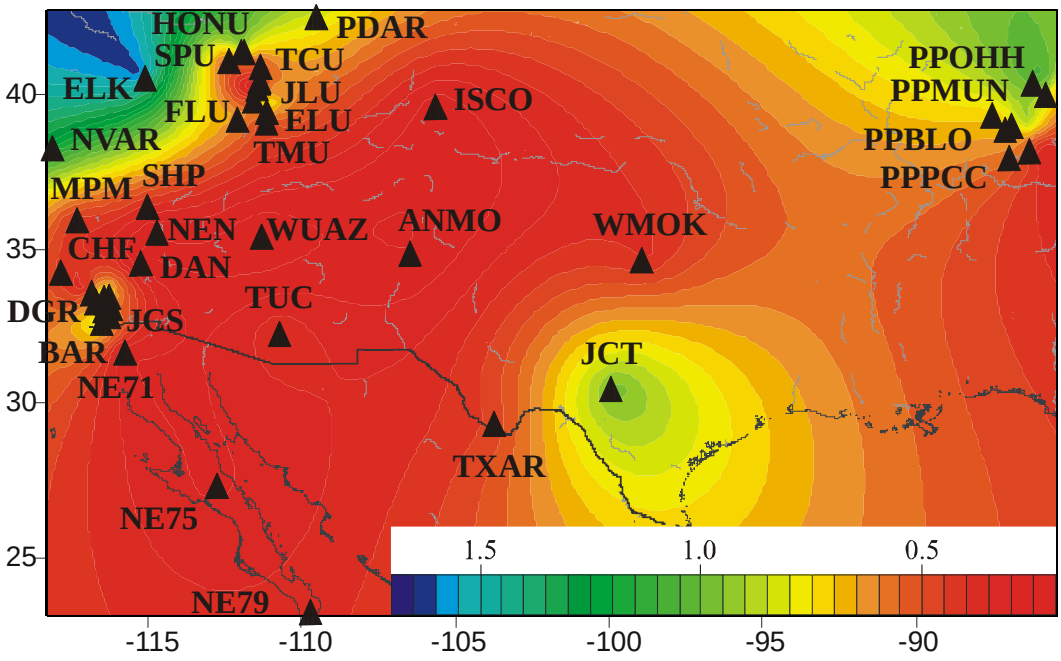

Fig. 10 Observed amplitude ratio values of PcP/P at the North American stations for 2002/10/12 event in West Brazil. Kriging interpolation with a medium smoothing.

	Region	Date	Time	Latitude	Longitude	Depth	Mag.
1	Fiji	1994/03/09	23:28:06.78	-18.04	-178.41	562	7.6
2	Argentina	1994/08/19	10:02:51.83	-26.44	-63.42	563	6.4
3	Tonga	1995/07/28	14:29:11.03	-21.18	-175.39	92	6.4
4	Bonin	1996/03/16	22:04:06.24	28.98	138.94	477	6.7
5	Fiji	1998/03/29	19:48:16.2	-17.55	-179.09	537.2	7.2
6	Fiji	2000/12/18	01:19:21.65	-21.2	-179.1	628	6.6
7	W. Brazil	2002/10/12	20:09:11.43	-8.3	-71.74	534	6.9
8	Fiji	2004/07/15	04:27:14.73	-17.66	-178.76	565	7.1

Table 1 NEIC event parameters used in this study.

Event	PKPab			P5KP		
	No. stations	Azimuth range (°)	Slowness (s/deg)	No. stations	Azimuth range (°)	Slowness (s/deg)
1994/03/09	21	340-352	3.89±0.41	21	340-352	4.70±0.21
1994/08/19	12	74-81; 44	4.23±0.07	19	74-81; 38-52	4.43±0.03
1995/07/28	16	345-353	4.04±0.21	16	345-353	4.35±0.20
1998/03/29	80	328-355	4.29±0.07	80	328-355	4.62±0.06
2000/12/18	15	303; 334-352	4.14±0.19	15	303; 334-352	4.35±0.48
2004/07/15	44	314-352	3.75±0.16	39	337-352	4.34±0.13
	ScP			P4KP		
2000/12/18	6	170-186	4.57±0.32	6	170-186	4.50±0.29
	PcP			P4KP		
2002/10/12	59	311-345	3.98±0.05	59	311-345	4.53±0.03

Table 2 Slowness estimations. Note that the estimations for P4KP and ScP slowness values at six South Pole stations provided close values.

Event	Station Δ (°)													
	Amplitude ratio P5KP vs PKP (x 100)													
	Obs.	Synt.												
1994/03/09	**GRA1** 147.4		**GRA4** 147.5		**WET** 147.6		**BFO** 149.2		**TTE** 150.6					
	0.89 ±0.10	0.27 ±0.03	0.57 ±0.08	0.26 ±0.03	0.30	0.29	0.58	0.35	0.69	0.37				
1994/08/19	**SP27** 155.5		**BB34** 155.8		**BB14** 156.6		**BB10** 156.8		**BB08** 156.9					
	0.69 ±0.14	0.53 ±0.04	0.72	0.53	1.74 ±0.12	0.70 ±0.13	0.71	0.59	0.52	0.57				
1995/07/28	**DPC** 149.4		**MOX** 150.0		**GRA1** 151.0		**GRB5** 151.2		**WET** 151.3		**GRA3** 151.9			
	0.56 ±0.03	0.32 ±0.02	0.94 ±0.11	0.31 ±0.02	1.06	0.38	1.24	0.43	1.86 ±0.21	0.43 ±0.11	0.77 ±0.10	0.37 ±0.01		
1998/03/29	**GRFO** 146.8		**WET** 147.0		**B35** 147.7		**FUR** 148.3		**BFO** 148.7		**BNI** 152.1		**AQU** 153.0	
	0.98	0.30	0.88 ±0.01	0.25 ±0.04	1.08 ±0.03	0.31	0.91 ±0.18	0.30 ±0.04	1.02 ±0.17	0.38	2.0 ±0.19	0.47 ±0.09	1.41 ±0.20	0.48

2000/12/18	**BSEG** 146.5		**CLL** 148.5		**IBBN** 148.5		**MORC** 148.5		**BRG** 148.6		**PSZ** 149.2		**TNS** 150.4		**WET** 150.5	
	0.81 ±0.10	0.26 ±0.03	0.64 ±0.05	0.44 ±0.06	1.55 ±0.05	0.34 ±0.04	0.92 ±0.15	0.30 ±0.04	0.48 ±0.02	0.34 ±0.02	0.78 ±0.17	0.45	0.82 ±0.02	0.42	0.83 ±0.02	0.42
2004/07/15	**WET** 147.2		**BFO** 148.8		**CEY** 149.9		**BOURR** 149.9									
	0.86 ±0.18	0.29	0.82 ±0.04	0.33	1.16 ±0.25	0.31 ±0.04	0.47 ±0.09	0.35								

Table 3 Amplitude ratio results (with 95% errors, where available) for P5KP vs PKPab.

Event	Station Δ (°)								
	Amplitude ratio P4KP vs P(S)cP (x 100)								
	Obs.	Synt.							
1996/03/16	**ASAR** 52.8		**ZRNK** 55.4						
	8.06 ±0.41	0.88 ±0.10	2.72 ±0.2	1.19					

2000/12/18	**ASAR** 43.3		**WRA** 43.5		*CBOB* 56.5		*DIHI* 59.4		*ISDE* 61.8		*JNCT* 56.9		*MBLO* 61.3		*VNDA* 57.1	
	1.06 ±0.03	0.63	1.76 ±0.04	0.61	7.80 ±0.39	0.78	7.65	1.38	7.43 ±0.42	1.88	7.38 ±0.78	0.84	6.59 ±0.33	1.50	9.74 ±0.62	1.02
2002/10/12	**ANMO** 54.2		**BAR** 59.2		**BMUT** 61.8		**DAN** 59.5		**DCU** 60.9		**DGR** 60.0		**DUG** 61.5		**ELK** 63.2	
	9.56 ±0.75	0.98	3.06 ±0.21	0. ±0.0	4.03 ±0.19	1.08 ±0.03	4.17 ±0.55	0. ±0.	5.45	1.02 ±0.17	2.32 ±0.16	1.22	7.20 ±0.13	1.60	9.76 ±0.13	1.26 ±0.13
	ELU 60.2		**EMU** 60.1		**FLU** 60.6		**FPU** 61.5		**FRD** 59.6		**GZU** 61.8		**HONU** 62.0		**IMU** 60.6	
	5.16	1.48	5.32 ±0.16	1.37	4.03 ±0.05	1.34	6.82 ±0.23	1.54	3.11 ±0.09	1.28	4.82 ±0.08	1.41	5.	1.32	7.34 ±0.08	1.42
	ISCO 57.3		**JCS** 59.4		**JCT** 47.2		**JLU** 61.0		**LVA2** 59.6		**MONP** 59.1		**MPM** 61.7		**MPU** 60.7	
	2.16 ±0.05	1.26	3.17 ±0.04	1.28	4.26 ±0.15	0.61 ±0.07	4.75 ±0.34	1.58	2.53 ±0.16	1.35	2.73 ±0.06	1.26	2.21 ±0.16	1.44	4.46 ±0.15	1.44
	NAIU 61.7		**NE71** 58.1		**NE75** 53.4		**NE79** 48.6		**NEN** 59.8		**NVAR** 63.6		**OWUT** 59.7		**PDAR** 61.5	
	4.60 ±0.22	1.43	3.69 ±0.28	1.10 ±0.07	2.21 ±0.10	0.93	3.8 ±0.46	0.95	3.5 ±0.04	1.45	0.84 ±0.02	1.55	5.27 ±0.52	1.42	1.76 ±0.06	1.55
	PLM 59.7		**PPBLO** 49.3		**PPEGH** 49.3		**PPMUN** 50.0		**PPNAF** 48.4		**PPNVW** 49.8		**PPOHH** 50.5		**PPPCC** 48.4	
	3.92 ±0.06	1.34	2.44 ±0.06	0.76 ±0.06	3.21 ±0.15	0.75 ±0.07	6.11 ±0.34	0.89	5.62 ±0.28	0.73 ±0.03	6.82 ±0.57	0.75 ±0.08	4.99 ±0.24	0.93	1.39 ±0.10	0.69
	RBU 61.3		**RCJ** 61.0		**RSUT** 61.7		**SAIU** 61.6		**SHP** 60.5		**SPU** 62.0		**SNUT** 61.8		**TCU** 61.3	

	4.16 ±0.14	1.36	8.89	1.46	2.85 ±0.06	1.43	5.65	1.65	2.69 ±0.19	1.32	6.62 ±0.27	1.32	4.98	1.35	2.83 ±0.05	1.40
	TCUT 61.3		**TM2** 60.0		**TMU** 60.0		**TRO** 59.5		**TUC** 55.0		**TXAR** 48.5		**WMOK** 50.0		**WMUT** 60.8	
	4.4	1.40	4.01 ±0.26	1.24	4.14 ±0.19	1.24	2.91 ±0.14	1.36	2.64 ±0.12	1.04	2.57 ±0.09	0.77	8.41 ±0.42	0.84	4.97 ±0.17	1.39
	WUAZ 49.9		**WVUT** 62.0		**YAQ** 59.2											
	3.96 ±0.24	1.14	4.02 ±0.20	1.30	2.95 ±0.14	1.16										

Table 4 Amplitude ratio results (with 95% errors, where available) for P4KP vs PcP. At the South Pole stations (Fig. 1), ScP is the reference phase.